Ain Shams Engineering Journal (2014) 5, 157–167

Ain Shams University

Ain Shams Engineering Journal

www.elsevier.com/locate/asej
www.sciencedirect.com

MECHANICAL ENGINEERING

MHD flow and heat transfer of an Ostwald–de Waele fluid over an unsteady stretching surface

K. Vajravelu [a], K.V. Prasad [b,*], P.S. Datti [c], B.T. Raju [d]

[a] Department of Mathematics, Department of Mechanical, Materials and Aerospace Engineering, University of Central Florida, Orlando, FL 32816, USA
[b] Department of Mathematics, VSK University, Vinayaka Nagar, Bellary 583 104, Karnataka, India
[c] T.I.F.R., Centre for Applicable Mathematics, Sharada Nagar, Yelahanka New Town, Bangalore 560 065, India
[d] Department of Mathematics, Bangalore University, Bangalore 560 001, India

Received 6 February 2013; revised 27 June 2013; accepted 31 July 2013
Available online 17 September 2013

KEYWORDS

Ostwald–de Waele fluid;
MHD flow;
Heat transfer;
Variable fluid properties;
Unsteady stretching surface;
Finite difference method

Abstract An analysis is carried out to study the effects of variable thermo-physical properties on an unsteady MHD flow and heat transfer of an Ostwald–de Waele fluid over a stretching surface. The thermo-physical properties, namely, viscosity and thermal conductivity of the fluid are assumed to vary with temperature. Using similarity transformation, the governing partial differential equations are converted into coupled, non-linear ordinary differential equations with variable coefficients. The resulting non-linear equations are solved numerically by a second-order finite difference scheme known as the Keller-box method for various values of the pertinent parameters. Also, the numerical results are obtained for special cases and are found to be in good agreement with those of the results available in the literature. Further, the results obtained reveal many interesting behaviors that warrant further study of the equations related to non-Newtonian fluid phenomena, especially the shear-thinning phenomena. Shear thinning reduces the wall shear stress.

1. Introduction

The fluid dynamics due to a stretching surface has gained interest in the recent past due to its technological applications in several engineering/industrial processes. Examples are numerous and they include the cooling of an infinite metallic plate in a cooling bath, the boundary layer along material handling conveyers, the aerodynamic extrusion of plastic sheets, paper production, glass blowing, metal spinning, drawing plastic films, and polymer extrusion. Sakiadis [1] was the first among the others to consider the boundary layer flow at a continuous solid surface with constant speed. Crane [2] extended the work of Sakiadis [1] to the flow caused by an elastic sheet moving in its own plane with a velocity varying linearly with the distance from a fixed point. This work was later extended by many authors [3–6] by considering the flow, heat, and mass transfer under different physical situations. These investigators, however, restricted their analyses to the flow of Newtonian fluids.

* Corresponding author. Tel.: +91 9448687862.
E-mail address: prasadkv2000@yahoo.co.in (K.V. Prasad).
Peer review under responsibility of Ain Shams University.

Production and hosting by Elsevier

2090-4479 © 2013 Production and hosting by Elsevier B.V. on behalf of Ain Shams University.
http://dx.doi.org/10.1016/j.asej.2013.07.009

Most of the fluids such as molten plastics, artificial fibers, petroleum, blood, and polymer solutions are considered as non-Newtonian fluids. Among several non-Newtonian models, the most popular rheological model for non-Newtonian fluid is the power-law or Ostwald–de Waele model. The power-law model provides an adequate representation of many non-Newtonian fluids over the most important range of shear rates. This together with its apparent simplicity has made it a very attractive model for both analytical and numerical research. The rheological equation of the state between the stress components τ_{ij} and strain components e_{ij} is defined by Vujannovic et al. [7],

$$\tau_{ij} = -p\delta_{ij} + K\left|\sum_{m=1}^{3}\sum_{l=1}^{3} e_{lm}e_{ml}\right|^{\frac{n-1}{2}} e_{ij}, \tag{1}$$

where p is the pressure, δ_{ij} is Kronecker delta, and K and n are, respectively, the consistency coefficient and the power-law index of the fluid. Andersson et al. [8] and Cortell [9] studied the boundary layer flow of an electrically conducting incompressible fluid obeying the power-law model in the presence of transverse magnetic field. Howell et al. [10] examined the momentum and heat transfer occurring in the laminar boundary layer on a continuously moving and stretching surface in a non-Newtonian power-law fluid. These studies dealt with stretching sheet where the flows were assumed to be steady. However, in reality, the flow and heat transfer can be unsteady due to a sudden stretching of the flat sheet or by a step change of the temperature of the sheet or when the surface is impulsively stretched with certain velocity, the flow is developed instantaneously. But, the flow in the viscous layer near the sheet is developed slowly, and it becomes fully developed steady flow after a certain time. Elbashbeshy and Bazid [11] presented a similarity solution for the boundary layer equations, which describe the unsteady flow and heat transfer over a stretching sheet and extended by Abd El-Aziz [12] for some physically realistic phenomena. Mukhopadhyay [13] analyzed the effect of variable fluid properties on the unsteady fluid flow and heat transfer over a stretching sheet in the presence of suction. Recently, a numerical study has been carried out by Sheikholeslami and Ganji [14], and Sheikholeslami et al. [15] on the modeling of natural convection heat transfer in nanofluids. The influence of chemical reaction on heat and mass transfer by natural convection from a vertical stretching surface was investigated theoretically by Abd El-Aziz and Salem [16]. But most of these studies are based on the constant thermo-physical properties of the ambient fluid. However, it is known [17] that these properties may change with temperature, especially the fluid viscosity and the thermal conductivity. To accurately predict the flow and heat transfer rates, it is necessary to take into account the variation of thermal conductivity and the viscosity. Available literatures [18–22] on the variable thermo-physical properties show that the effects of variable fluid properties have not been investigated for unsteady non-Newtonian Ostwald–de Waele fluid over a stretching sheet.

Motivated by these investigations and their applications, in the present article, the authors examine the effects of the variable fluid properties on the MHD flow and heat transfer of Ostwald–de Waele fluid induced by an accelerating unsteady stretching sheet in the presence of viscous dissipation and internal heat generation/absorption. The governing non-linear partial differential equations of the problem are transformed into a system of non-linear, coupled ordinary differential equations with variable coefficients. The system of equations with the appropriate boundary conditions are solved numerically by an implicit finite difference scheme known as the Keller-box method for several sets of values of the physical parameters. Typical results for the temperature and velocity profiles, skin friction and wall-temperature gradient are presented through graphs and tables for several sets of values of the governing parameters. Also, the numerical results for the skin friction and the wall-temperature gradient are compared with the available results in the literature for different values of Mn and n in the absence of thermo-physical properties and are found to be in very good agreement.

2. Mathematical formulation

Consider the flow of an unsteady two-dimensional flow of an incompressible viscous homogenous electrically conducting non-Newtonian power-law fluid obeying Ostwald–de Waele model past an impermeable long continuous sheet which is being issued from a slot (shown in Fig. 1) coinciding with the plane $y = 0$ and the flow being confined to $y > 0$. The moving of the continuous sheet is taken up by a wind-up roll. The assumption is also made that a certain time has elapsed after the initiation of motion, so that steady state condition prevails. Any flow disturbance created by the roll is neglected. An observer fixed in space will note that the boundary layer on the sheet originates at the slot and grows in the direction of the motion of the sheet. The origin is located at the slit through which the sheet is drawn through the fluid medium, the x-axis is taken in the direction of the flow along the sheet and y-axis is normal to it. Two equal and opposite forces are applied along the x-axis, so that the sheet is stretched, keeping the origin fixed. The continuous sheet assumed to vary with a velocity U_w and having a prescribed surface temperature T_w at the solid surface, and the fluid moves in the x-direction with a velocity (u-component) equal to the velocity of the solid surface, whereas at increasing distance from the surface, the velocity of the fluid in the x-direction approaches to zero asymptotically. It is envisaged that the flow approaches the sheet with zero angle of incidence and the sheet issues from a slot at the origin. The velocity and the temperature of the plate are assumed to be

$$U_w = bx/(1 - \alpha t), \tag{2}$$

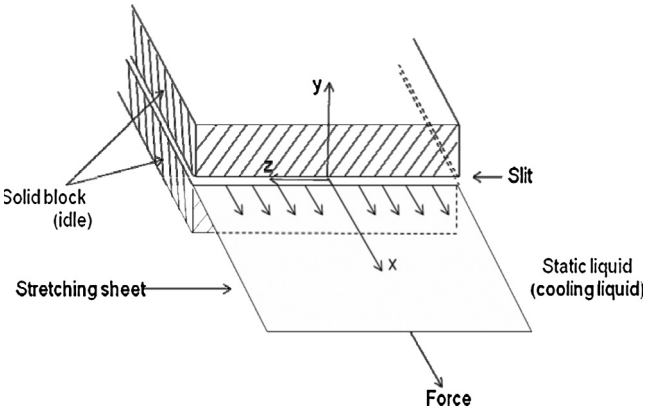

Figure 1a Schematic of an extrusion processes.

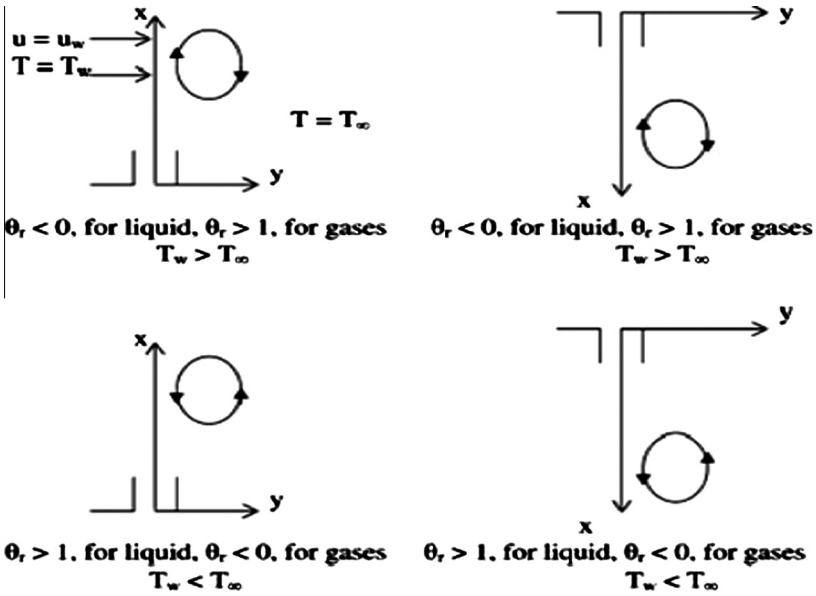

Figure 1b Schematic of an extrusion processes and different physical situations.

$$T_w = T_\infty + (1-\alpha t)^{n-\frac{5}{2}} b^{2-n}/2\gamma_\infty, \tag{3}$$

where b and α are positive constants, n is the power-law index, $bx/(1-\alpha t)$ is the effective stretching and T_w is the sheet temperature. It is apparent to note that the above expressions are valid for time $t < 1/\alpha$. The thermo-physical fluid properties are assumed to be isotropic and constant, except for the fluid viscosity and the fluid thermal conductivity which are assumed to vary as a function of temperature as follows:

$$\frac{1}{\mu} = \frac{1}{\mu_\infty}[1+\delta(T-T_\infty)], \tag{4}$$

$$k(T) = k_\infty\left[1+\varepsilon\frac{T-T_\infty}{\Delta T}\right], \tag{5}$$

where μ_∞ and k_∞ are respectively the ambient viscosity and the thermal conductivity of the fluid. $\varepsilon = (k_w - k_\infty)/k_\infty$ is known as the variable thermal conductivity parameter, T is the temperature of the fluid, and $\Delta T = T_w - T_\infty$ is the temperature difference. Eq. (4) can be written as

$$\frac{1}{\mu} = a(T-T_r), \tag{6}$$

$$\text{where} \quad a = \frac{\delta}{\mu_\infty} \quad \text{and} \quad T_r = T_\infty - \frac{1}{\delta}, \tag{7}$$

with a and T_r are being constants and their values depend on the reference state and the thermo-physical property of the fluid, i.e., δ: In general, $a > 0$ for liquids and $a < 0$ for gases. Also, θ_r, is a constant which is defined by

$$\theta_r = \frac{T_r - T_\infty}{\Delta T} = -\frac{1}{\delta\Delta T}. \tag{8}$$

It is worth mentioning here that when $\delta \to 0$, i.e., $\mu = \mu_\infty$ (constant), then $\theta_r \to \infty$. It is also important to note that θ_r is negative for liquids and positive for gases when $(T_w - T_\infty)$ is positive (see [18]). This is due to the fact that the viscosity of the liquid usually decreases with increasing temperature, while it increases for gases. The flow region is exposed under the influence of an external magnetic field of strength B_0 in the positive y-direction, which is assumed to be variable and is chosen in the special form as

$$B_0(t) = B_0(1-\alpha t)^{-1/2}. \tag{9}$$

This form of $B_0(t)$ has also been considered by Anjali Devi and Thyagarajan [6] while analyzing the MHD flow over an unsteady stretching surface. The induced magnetic field is negligible, which is a valid assumption on a laboratory scale under the assumption of small Reynolds number and zero external electric field. Under these assumptions and the usual boundary layer approximations, the velocity and the temperature fields of the non-Newtonian Ostwald–de Waele fluid are governed by the following equations of mass, momentum, and energy:

$$\frac{\partial u}{\partial x} + \frac{\partial}{\partial y} = 0, \tag{10}$$

$$\frac{\partial u}{\partial t} + u\frac{\partial u}{\partial x} + \frac{\partial u}{\partial y} = \frac{\partial}{\partial y}\left(\frac{1}{\rho_\infty}\tau_{xy}\right) - \frac{\sigma B_0^2(t)}{\rho_\infty}u, \tag{11}$$

$$\frac{\partial T}{\partial t} + u\frac{\partial T}{\partial x} + \frac{\partial T}{\partial y} = \frac{1}{\rho_\infty c_p}\frac{\partial}{\partial y}\left(k(T)\frac{\partial T}{\partial y}\right) + \frac{Q}{\rho_\infty c_p}(T-T_\infty) + \frac{\mu(T)}{\rho_\infty c_p}\left(\frac{\partial u}{\partial y}\right)^{n+1}, \tag{12}$$

where u and are the velocity components along the x- and y-directions respectively, ρ_∞ is the density, and τ_{xy} is the shear stress. The shear stress is given by

$$\frac{\tau_{xy}}{\rho_\infty} = -\mu\left(-\frac{\partial u}{\partial y}\right)^n = \frac{\mu_\infty}{[1+\delta(T-T_\infty)]}\left(-\frac{\partial u}{\partial y}\right)^n, \tag{13}$$

where μ is the absolute viscosity, μ_∞ is the dynamic viscosity of the ambient fluid, and n is the power-law index. As n deviates from unity, the fluid becomes non-Newtonian: For example, $n < 1$ and $n > 1$ corresponding to shear thinning (pseudo plastic) and shear thickening (dilatants) fluids respectively, and for $n = 1$, it is simply the Newtonian fluid. Several fluids studied in the literature fall into the range of $0 < n \leqslant 2$. The

term in the right hand side of Eq. (13), i.e., the shear rate ($\partial u/\partial y$) has been assumed to be negative throughout the entire boundary layer, since the stream-wise velocity component u decreases monotonically with the distance y from the moving surface. A rigorous derivation and subsequent analysis of the boundary layer equations for power-law fluids were recently provided by Denier and Dabrowski [23]. They focused on boundary layer flow driven by free stream $U(x) \approx x^m$ which is of the Falkner–Skan type. Such boundary layer flows are driven by a stream wise pressure gradient $-\frac{dp}{dx} = \rho\frac{dU}{dx}$, set up by the external free stream outside the viscous boundary layer. In the present context, no driving pressure gradient is present. Instead, the flow is driven solely by a flat surface which moves with a prescribed velocity U_w and σ is the electrical conductivity. In Eq. (12), T is the temperature, c_p is the specific heat at constant pressure, and $k(T)$ is the temperature dependent variable thermal conductivity (Eq. (5)). For liquid metals, the thermal conductivity varies linearly with temperature in the range 0–400 °F [21]. The term containing Q in Eq. (12) represents the temperature-dependent volumetric rate of heat source when $Q > 0$ and heat sink when $Q < 0$: These deal with the situation of exothermic and endothermic chemical reactions, respectively. Substituting (2)–(9) into the (11), (12), we obtain

$$\frac{\partial u}{\partial t}+u\frac{\partial u}{\partial x}+\frac{\partial u}{\partial y}=-\mu_\infty\frac{\partial}{\partial y}\left(\frac{1}{[1+\delta(T-T_\infty)]}\left(-\frac{\partial u}{\partial y}\right)^n\right)-\frac{\sigma B_0^2(t)}{\rho_\infty}u, \tag{14}$$

$$\frac{\partial T}{\partial t}+u\frac{\partial T}{\partial x}+\frac{\partial T}{\partial y}=\frac{1}{\rho_\infty c_p}\frac{\partial}{\partial y}\left(k_\infty\left(1+\varepsilon\frac{T-T_\infty}{\Delta T}\right)\frac{\partial T}{\partial y}\right)+\frac{Q}{\rho_\infty c_p}(T-T_\infty)+\frac{\mu_\infty}{\rho_\infty c_p}\times\frac{1}{[1+\delta(T-T_\infty)]}\left(\frac{\partial u}{\partial y}\right)^{n+1}. \tag{15}$$

The appropriate boundary conditions are

$$u = U_w \quad = 0 \quad T = T_w \quad \text{at } y = 0, \tag{16}$$

$$u \to 0, \quad T \to T_\infty \quad \text{as } y \to \infty, \tag{17}$$

where U_w and T_w are the surface velocity and temperature of the stretching sheet, respectively. We introduce the following dimensionless variable $f(\xi)$ and $\theta(\xi)$ as well as the similarity variable ξ as

$$\psi = (b^{1-2n}/\gamma_\infty)^{\frac{-1}{n+1}}x^{\frac{2n}{n+1}}(1-\alpha t)^{\frac{1-2n}{n+1}}f(\xi), \tag{18}$$

$$T = T_\infty + (T_w - T_\infty)\,\theta(\xi), \tag{19}$$

$$\xi = (b^{2-n}/\gamma_\infty)^{\frac{1}{n+1}}x^{\frac{1-n}{n+1}}(1-\alpha t)^{\frac{n-2}{n+1}}y. \tag{20}$$

In Eq. (18), the stream function $\psi(x, y, t)$ is defined by $u = \partial\psi/\partial y$ and $= -\partial\psi/\partial x$, such that the continuity Eq. (10) is satisfied automatically (here, $\gamma_\infty = \mu_\infty/\rho_\infty$ is the kinematic viscosity, and $\alpha_\infty = k_\infty/\rho_\infty C_p$ is the thermal diffusivity). In terms of these new variables, the momentum and the energy equations together with the boundary conditions become

$$\left(\frac{2n}{n+1}ff''-f'^2\right)-\left((-f'')^n\left(1-\frac{\theta}{\theta_r}\right)^{-1}\right)'-A\left(f'+\frac{2-n}{n+1}\xi f''\right)-Mnf'=0, \tag{21}$$

$$((1+\varepsilon\theta)\theta')'-A\,Pr\left[\left(\frac{5}{2}-n\right)\theta+\frac{2-n}{n+1}\xi\theta'\right]+PrEc\left(1-\frac{\theta}{\theta_r}\right)^{-1}(f'')^{n+1}+Pr\left(\frac{2n}{n+1}f\theta'+\beta\theta\right)=0, \tag{22}$$

and

$$f(0)=0, \quad f'(0)=1, \quad f'(\infty)=0, \tag{23}$$

$$\theta(0)=1, \quad \theta(\infty)=0, \tag{24}$$

where prime denotes differentiation with respect to ξ, and $\theta_r = -1/\delta(T_w - T_\infty)$ is the fluid viscosity parameter. It is important to note that larger value of θ_r implies that δ or $(T_w - T_\infty)$ is small, and the effects of variable viscosity can thus neglected. On other hand, for a smaller value of θ_r either the fluid viscosity change markedly with temperature or the operating temperature difference is high. In either case, the variable viscosity effect is expected to become very important. Further, $A = \alpha/b$ is the dimensionless measure of the unsteadiness, $Mn = \sigma B_0^2/\rho_\infty b$ is the magnetic parameter, $P_r = (U_w/\alpha_\infty)Re_x^{-2/(n+1)}$ is the generalized Prandtl number for power-law fluids, $E_c = U_w^2/C_p(T_w - T_\infty)$ is the Eckert number and $\beta = Q/\rho_\infty c_p b$ is the heat source/sink parameter. It is worth mentioning here that the momentum boundary layer problem defined by the ODE (21) subject to the boundary conditions (23) is de-coupled from the thermal boundary layer problem, while the temperature field is on the other hand coupled with the velocity field. Further, for a Newtonian fluid with constant thermal conductivity $n = 1$, $\varepsilon = 0$, $A = 0$ and $\theta_r \to \infty$, Eqs. (20) and (21) reduce to those of Anjali Devi and Thyagarajan [6]. However, for the non-Newtonian power-law fluids, when there is no heat transfer, Eq. (21) reduces to that of Andersson et al. [8]. Further, when the unsteady parameter and the Eckert number are absent, and $\theta_r \to \infty$, Eqs. (21) and (22) are similar to the ones studied by earlier researchers for Newtonian fluid case. For practical purposes, the physical quantities of interest include the velocity components u and , the local skin friction coefficient C_{fx}, and the local Nusselt number Nu_x. These physical quantities can be written as

$$u = U_w f', \quad = -U_w\,Re_x^{\frac{-2}{n+1}}\left[\frac{2n}{n+1}f+\frac{1-n}{1+n}\xi f'\right], \tag{25}$$

$$C_{fx} = \frac{2\tau_{xy}}{\rho_\infty U_w^2} = \frac{2\theta_r}{\theta_r-1}Re_x^{\frac{-1}{n+1}}[-f''(0)]^n, \quad Nu_x = \frac{1}{2}(1-\alpha t)^{-\frac{1}{2}}Re_x^{\frac{n+2}{n+1}}\theta'(0), \tag{26}$$

where $Re_x = U_w^{2-n}x^n/\gamma_\infty$ and $\frac{\tau_{xy}}{\rho_\infty} = \mu\left(\frac{\partial u}{\partial y}\right)_{at y=0}$ are the local Reynolds number and the shear stress, respectively.

3. Numerical procedure

By using a similarity transformation, the governing equations of the problem are reduced to a system of coupled, non-linear ordinary differential equations, which are solved numerically by the Keller-box method [24]. This method is unconditionally stable and has a second order accuracy with arbitrary spacing. The numerical solutions can be obtained in the following four steps:

- Reduce Eqs. (21) and (22) to a system of first-order equations;
- Write the difference equations using central differences;
- Linearize the algebraic equations by Newton's method, and write them in matrix–vector form; and
- Solve the linear system by the block tri-diagonal elimination technique.

For the sake of brevity, further details of the solution process are not presented here. It is also important to note that the computational time for each set of parametric values should be short. The physical domain of the problem is unbounded, whereas the computational domain is finite, we apply the far field boundary conditions for the similarity variable ξ at a finite value denoted by ξ_{max}. We ran bulk of our computations with the value $\xi_{max} = 8$ which is sufficient to achieve the far field boundary conditions asymptotically for all values of the parameters considered. For numerical calculations, a uniform step size of $\Delta\xi = 0.01$ is found to be satisfactory and the solutions are obtained with an error tolerance of 10^{-6} in all cases. To assess the accuracy of the present method, comparison of the skin friction and the wall-temperature gradient between the present results and the previously published results are made, for several special cases (see Tables 1 and 2) and found very good agreement.

4. Results and discussion

Numerical computations are carried out for several sets of values of the governing parameters, namely, the unsteady parameter A, the power-law index parameter n, the magnetic parameter Mn, the variable thermal conductivity parameter ε, the heat source/sink parameter β, the fluid viscosity parameter θ_r, the Prandtl number Pr, and the Eckert number Ec. In order to illustrate the salient features of the flow and heat transfer phenomena, the numerical results are presented in Figs. 2–8. These figures depict the changes in the horizontal fluid velocity and the fluid temperature distribution. Variations in the skin friction and the wall-temperature gradient for several sets of the pertinent parameters are recorded in Table 3.

The horizontal velocity profiles f' are shown graphically in Figs. 2a–2d for different values of A, Mn, n, and θ_r. The general trend is that f' decreases monotonically as the distance increases from the slit. The effect of increasing values of the fluid viscosity parameter θ_r is to decrease the momentum boundary layer thickness. Also, as $\theta_r \to 0$, the boundary layer thickness decreases and the velocity distribution asymptotically tends to zero (see Figs. 2a and 2b). This is due to the fact that, for a given fluid, when δ is fixed, smaller θ_r implies higher temperature difference between the wall and the ambient fluid. The results presented in this paper demonstrate clearly that θ_r,

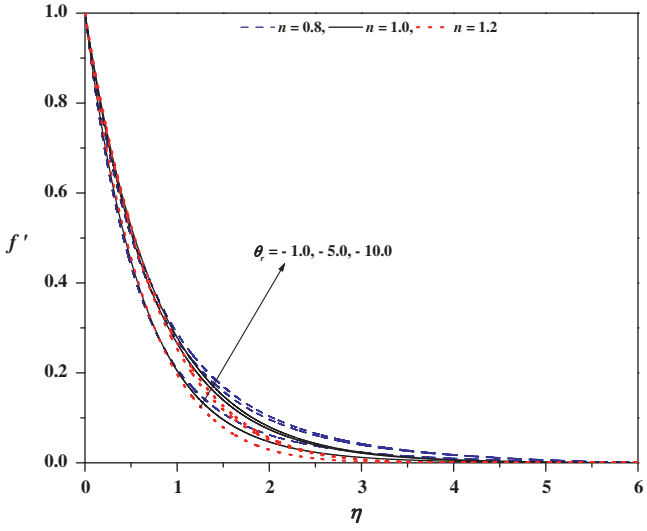

Figure 2a Horizontal velocity profiles for different values of n and θ_r with $\varepsilon = 0.01$, $Ec = 0.01$, $Mn = 0.5$, $Pr = 1.0$, $\beta = -0.1$ when $A = 0.0$.

Table 1 Numerical results of skin friction coefficient $f''(0)$ for different values of Mn and n in the absence of thermo-physical properties.

Mn	Present work			Andersson et al. [8]			Prasad et al. [20]		
	$n = 0.8$	$n = 1.0$	$n = 1.2$	$n = 0.8$	$n = 1.0$	$n = 1.2$	$n = 0.8$	$n = 1.0$	$n = 1.2$
0.0	−1.034639	−1.000149	−0.987454	−1.034	−1.000	−0.989	−1.03400	−1.00000	−0.98900
0.5	−1.308875	−1.224930	−1.175000	−1.308	−1.224	−1.175	−1.30860	−1.22490	−1.17520
1.0	−1.544365	−1.414249	−1.333021	−1.544	−1.414	−1.333	−1.54429	−1.41440	−1.33306
1.5	−1.754095	−1.581153	−1.471513	−1.754	−1.581	−1.471	−1.75406	−1.58100	−1.47150
2.0	−1.945368	−1.732062	−1.596003	−1.945	−1.732	−1.595	−1.94588	−1.73200	−1.59599

Table 2 Comparison of wall-temperature gradient $\theta'(0)$ for different values of the Prandtl number Pr when $Ec = \varepsilon = \beta = A = Mn = 0.0$ and $\theta_r \to -\infty$.

Pr	Present work	Grubka and Bobba [4]	Chen [5]	Ali [19]
0.72	−0.463146	−0.4631	−0.46315	−0.4617
1.0	−0.583693	−0.5820	−0.58199	−0.5801
3.0	−1.165171	−1.1652	−1.16523	−1.1599
10.0	−2.307920	−2.3080	−2.30796	−2.2960
100.0	−7.769591	−7.7657	–	–

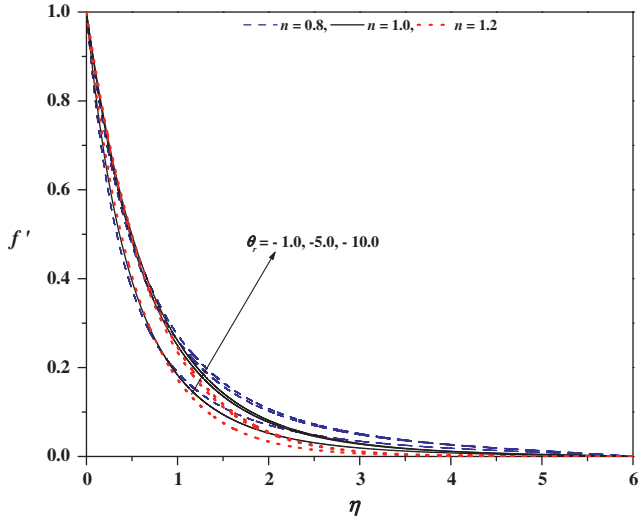

Figure 2b Horizontal velocity profiles for different values of n and θ_r with $\varepsilon = 0.01$, $Ec = 0.01$, $Mn = 0.5$, $Pr = 1.0$, $\beta = -0.1$ when $A = 0.5$.

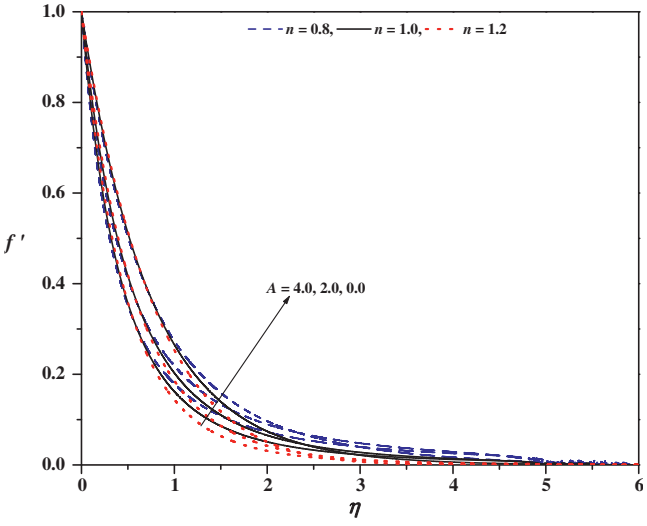

Figure 2c Horizontal velocity profiles for different values of n and A with $\varepsilon = 0.01$, $Ec = 0.01$, $Mn = 0.5$, $Pr = 1.0$, $\beta = -0.1$ when $\theta_r = -5.0$.

the indicator of the variation of fluid viscosity with temperature, has a substantial effect on the horizontal velocity f' and hence on the skin friction. Further, the effect of increasing values of the unsteady parameter A is to decrease f'. The effect of increasing power-law index parameter n is to reduce the horizontal velocity and thereby reduces the boundary layer thickness, i.e., the thickness is much larger for shear thinning (pseudo plastic) fluids ($0 < n < 1$) than that of the Newtonian fluid ($n = 1$); and the shear thickening (dilatant) fluids ($1 < n < 2$), as clearly seen from Fig. 2c. The effect of the magnetic parameter Mn on the horizontal velocity profile is to decrease it. That is, an increase in the magnetic parameter has a tendency to create a drag, known as the Lorentz force, which tends to resist the flow. This behavior is true even in the case of shear thickening and shear thinning fluids (see Fig. 2d).

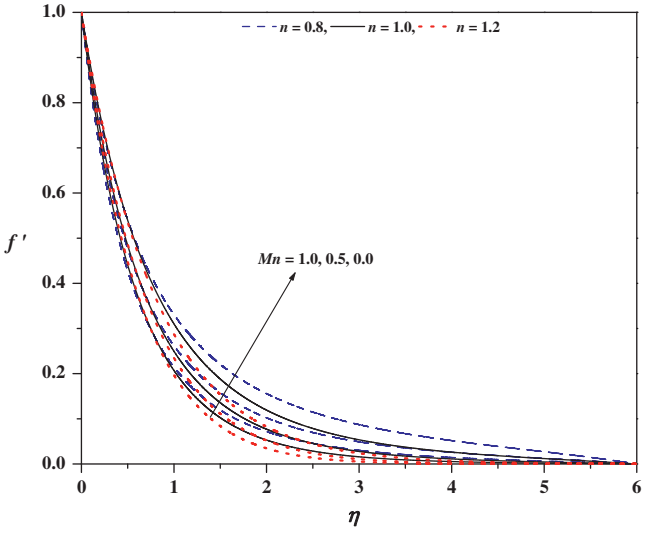

Figure 2d Horizontal velocity profiles for different values of n and Mn with $\varepsilon = 0.01$, $Ec = 0.01$, $Pr = 1.0$, $\beta = -0.1$, $\theta_r = -5.0$ when $A = 0.5$.

In Figs. 3–8, the numerical results for the temperature $\theta(\xi)$ for several sets of values of the governing parameters are presented. The general trend is that the temperature distribution is unity at the wall. However, the temperature distribution tends asymptotically to zero as $\xi \to \infty$ for all values of the governing parameters. Figs. 3a and 3b, respectively, exhibit the combined effects of the power-law index and the fluid viscosity parameter on the temperature profiles for both the cases, namely, zero and non-zero values of an unsteady parameter. The effect of increasing values of the power-law index n leads to thinning of the thermal boundary thickness. This behavior is very much noticeable in shear thinning and shear thickening fluids. Further, from Figs. 3a and 3b, we notice that the effect of increasing values of the fluid viscosity parameter θ_r is to enhance the

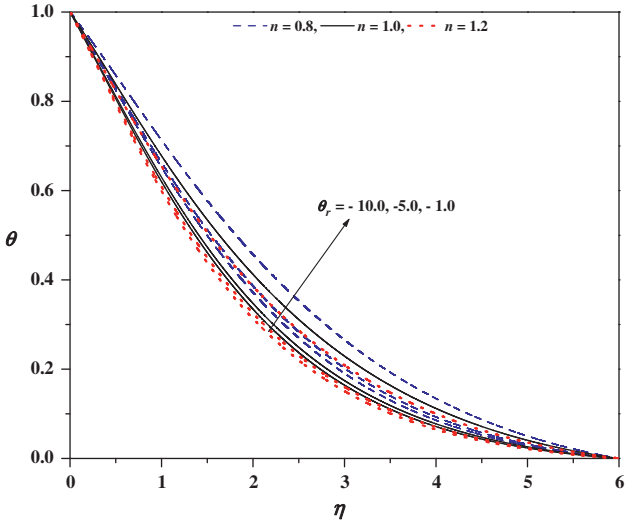

Figure 3a Temperature profiles for different values of n and θ_r with $\varepsilon = 0.01$, $Ec = 0.01$, $Mn = 0.5$, $Pr = 1.0$, $\beta = -0.1$ when $A = 0.0$.

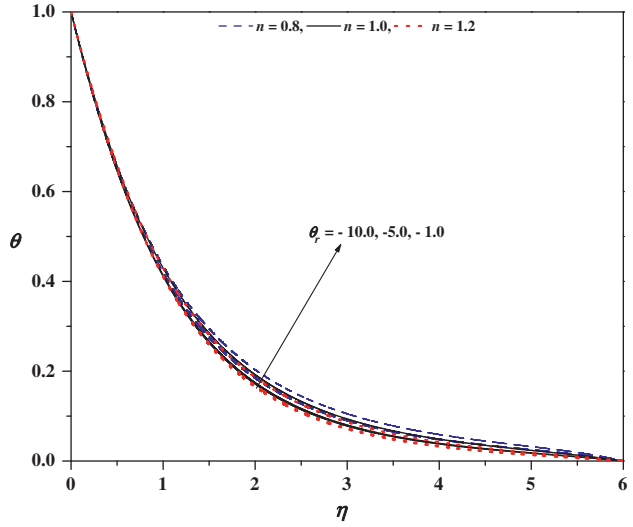

Figure 3b Temperature profiles for different values of n and θ_r with $\varepsilon = 0.01$, $Ec = 0.01$, $Mn = 0.5$, $Pr = 1.0$, $\beta = -0.1$ when $A = 0.5$.

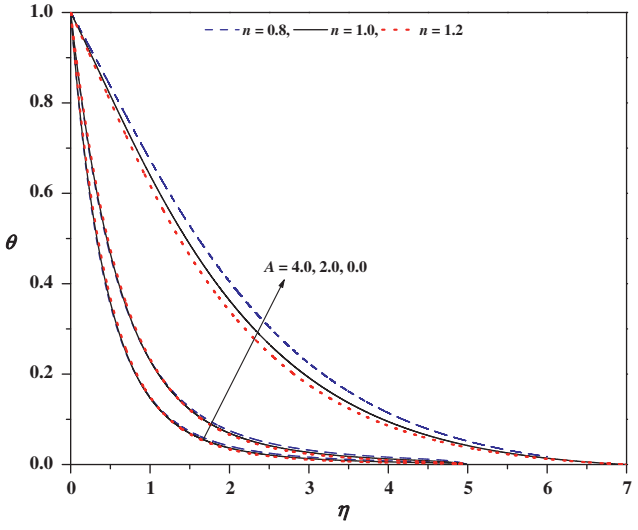

Figure 3c Temperature profiles for different values of n and A with $\varepsilon = 0.01$, $Ec = 0.01$, $Mn = 0.5$, $Pr = 1.0$, $\beta = -0.1$ when $\theta_r = -5.0$.

temperature. This is even true in the presence of non-zero values of the unsteady parameter. This is due to the fact that an increase in the fluid viscosity parameter θ_r results in an increase in the thermal boundary layer thickness. Further, the effect of increasing values of unsteady parameter A is to reduce the temperature and hence reduces the thermal boundary layer thickness (see Fig. 3c), whereas the effect of the magnetic parameter is to enhance the temperature (Fig. 3d). This is because of the fact that when a transverse magnetic field is applied to an electrically conducting fluid gives rise a resistive force, known as the Lorentz force. This force makes the fluid to experience a resistance by increasing the friction between its layers and due to which there is an increase in the value of the temperature in the boundary layer.

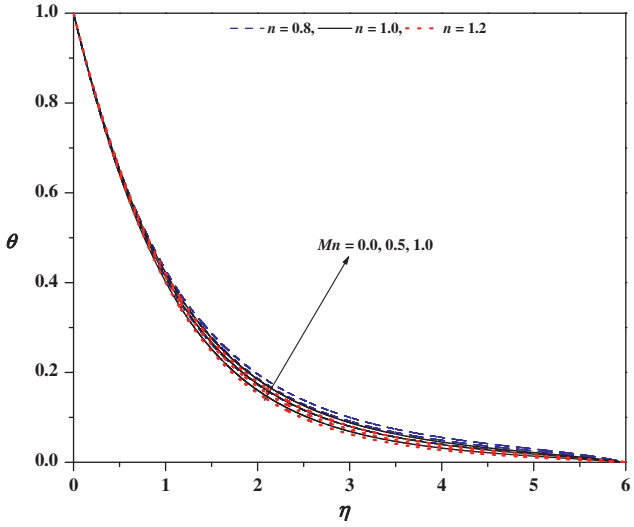

Figure 3d Temperature profiles for different values of n and Mn with $\varepsilon = 0.01$, $Ec = 0.01$, $Pr = 1.0$, $\beta = -0.1$, $\theta_r = -5.0$ when $A = 0.5$.

The effects of variable thermal conductivity parameter ε on the temperature profile $\theta(\xi)$ in the boundary layer for different types of fluids, namely, shear thinning, Newtonian and shear thickening fluids are shown graphically in Fig. 4. From the graphical representation, we observe that the temperature distribution is lower throughout the boundary layer for zero values of ε as compared with non-zero values of ε. This is due to the fact that the presence of temperature-dependent thermal conductivity results in reducing the magnitude of the transverse velocity by a quantity $\partial k(T)/\partial y$, and this can be seen from the energy equation. The graphs for the temperature distribution $\theta(\xi)$ for various values of the Prandtl number Pr and the power-law index n are plotted in Fig. 5. From the graphs, we observe that an increase in Pr results in a monotonic decrease in the temperature distribution and it tends to zero as the distance increases from the elastic sheet. It is noteworthy that

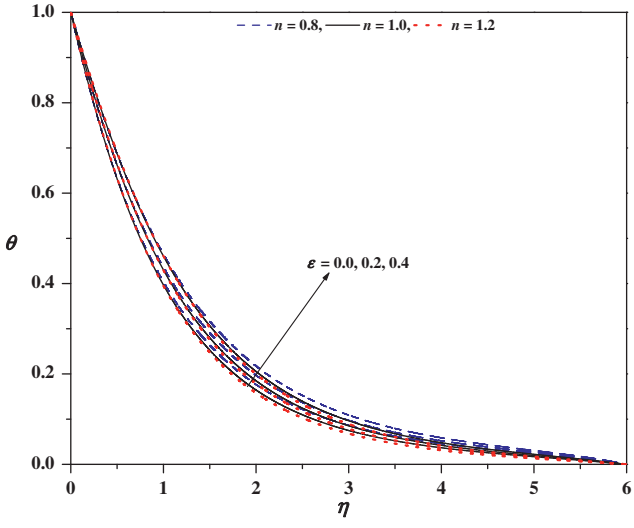

Figure 4 Temperature profiles for different values of n and ε with $Ec = 0.01$, $Mn = 0.5$, $Pr = 1.0$, $\beta = -0.1$, $\theta_r = -1.0$ when $A = 0.5$.

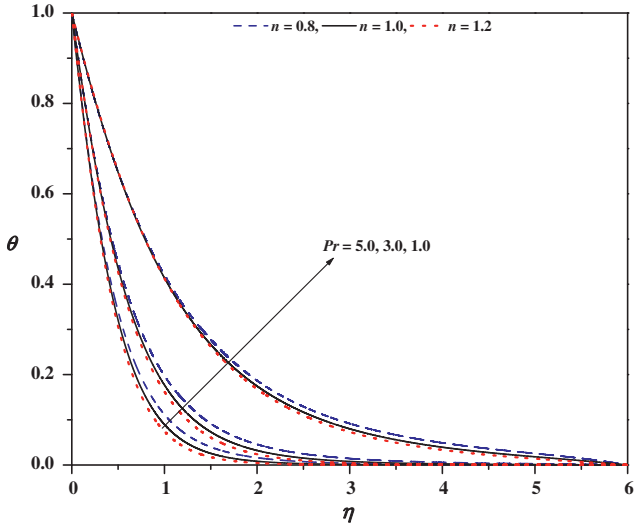

Figure 5 Temperature profiles for different values of n and Pr with $\varepsilon = 0.01$, $Ec = 0.01$, $Mn = 0.5$, $\beta = -0.1$, $\theta_r = -5.0$ when $A = 0.5$.

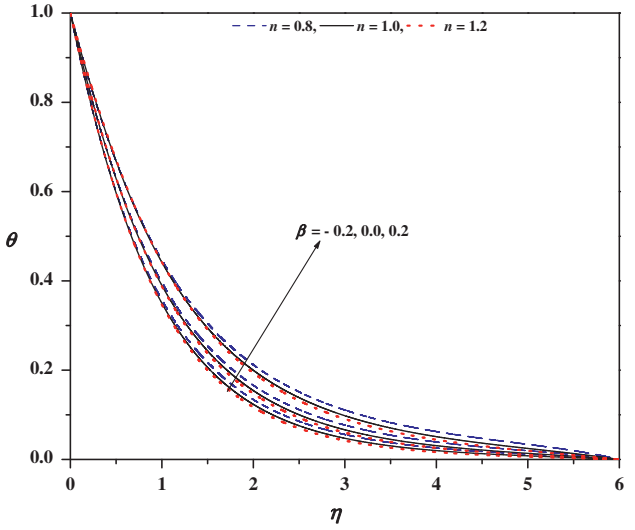

Figure 7 Temperature profiles for different values of n and β with $\varepsilon = 0.1$, $Ec = 0.01$, $Pr = 1.0$, $Mn = 0.5$, $\theta_r = -5.0$ when $A = 0.5$.

the temperature vanishes at the free surface for sufficiently larger values of the Prandtl number. This is analogs to the situation in a steady/unsteady state aerodynamic boundary layer in an infinite fluid medium at high Prandtl number. That is, the thermal boundary layer thickness decreases for higher values of the Prandtl number. This holds good for all values of power-law index n.

Fig. 6 depicts the temperature distribution $\theta(\xi)$ for different values of Ec. An increase in the value of Ec is to increase the temperature distribution $\theta(\xi)$. This is in conformity with the fact that energy is stored in the fluid region as a consequence of dissipation due to viscosity and elastic deformation. Fig. 7 exhibits the temperature distribution $\theta(\xi)$ for different values of heat source/sink parameter β for all fluids considered here, namely, shear thinning, Newtonian and shear thickening fluids. From this figure, we observe that the temperature distribution is lower throughout the boundary layer for negative values of β (heat sink) and higher for positive values of β (heat source). Physically $\beta > 0$ implies $T_w > T_\infty$, i.e., there will be a supply of heat to the flow region from the wall. Similarity $\beta < 0$ implies $T_w < T_\infty$ and there will be a transfer of heat from the flow to the wall. The effect of increasing the values of the heat source/sink parameter β is to increase the temperature profile $\theta(\xi)$. However, minimum temperature distribution is observed in shear thickening as compared to Newtonian or Shear thinning fluids.

Numerical results for the skin friction coefficient $f''(0)$ and the Nusselt number $\theta'(0)$, as a function of unsteady parameter

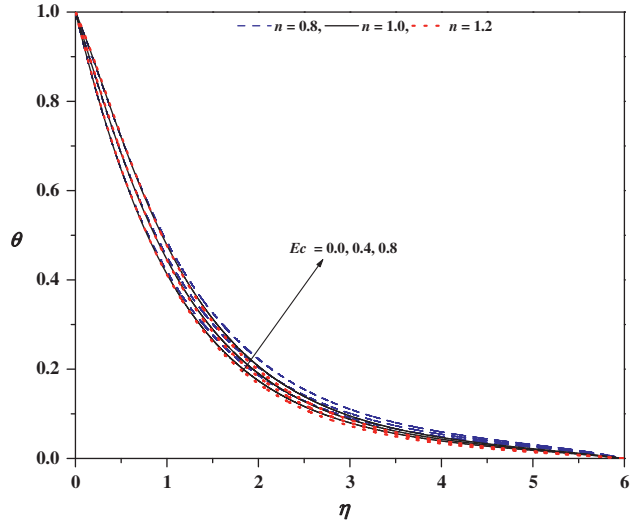

Figure 6 Temperature profiles for different values of n and Ec with $Mn = 0.5$, $\varepsilon = 0.1$, $Pr = 1.0$, $\beta = -0.1$, $\theta_r = -5.0$ when $A = 0.5$.

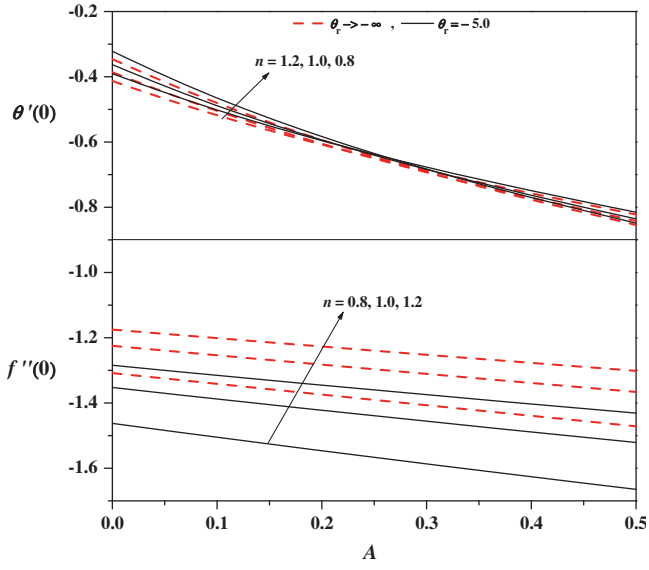

Figure 8 Values of $f''(0)$ and $\theta'(0)$ for different values of θ_r and n with $\varepsilon = 0.01$, $Ec = 0.01$, $Mn = 0.5$, $Pr = 1.0$, $\beta = -0.1$.

Table 3 Values of the skin friction coefficient $f''(0)$ and wall-temperature gradient $\theta'(0)$ for different values of the pertinent parameters.

Pr	Ec	ε	Mn	β	θ_r	$A = 0.0$						$A = 0.5$					
						$n = 0.8$		$n = 1.0$		$n = 1.2$		$n = 0.8$		$n = 1.0$		$n = 1.2$	
						$f''(0)$	$\theta'(0)$	$f''(0)$	$\theta'(0)$	$f''(0)$	$\theta'(0)$	$f''(0)$	$\theta'(0)$	$f''(0)$	$\theta'(0)$	$f''(0)$	$\theta'(0)$
1.0	0.01	0.1	0.5	−0.1	$\to-\infty$	−1.308347	−0.345998	−1.224784	−0.386147	−1.174995	−0.413076	−1.471440	−0.854360	−1.366251	−0.842011	−1.301526	−0.822276
					−10.0	−1.389185	−0.333382	−1.291658	−0.374005	−1.232347	−0.401299	−1.571808	−0.851401	−1.446702	−0.838686	−1.368960	−0.818609
					−5.0	−1.462511	−0.321764	−1.352355	−0.362743	−1.284386	−0.390341	−1.664808	−0.848713	−1.520986	−0.835652	−1.431030	−0.815251
					−1.0	−1.730448	−0.264116	−1.596360	−0.306524	−1.504302	−0.336094	−2.397510	−0.828837	−2.079934	−0.814239	−1.879483	−0.792387
1.0	0.01	0.1	0.5	−0.2	−5.0	−1.476070	−0.627410	−1.361122	−0.654401	−1.290613	−0.674481	−1.670803	−0.999425	−1.255198	−0.990221	−1.434228	−0.974666
				0.0		−1.468365	−0.448054	−1.356101	−0.481933	−1.287035	−0.505920	−1.666984	−0.902082	−1.522524	−0.890643	−1.432206	−0.872266
				0.2		−1.453136	−0.131840	−1.346511	−0.188473	−1.280288	−0.223179	−1.662398	−0.791254	−1.519263	−0.775997	−1.429699	−0.752865
1.0	0.01	0.1	0.0	−0.1	−5.0	−1.159280	−0.387501	−1.107704	−0.422914	−1.081135	−0.443522	−1.389074	−0.861939	−1.302222	−0.850018	−1.251319	−0.830160
			0.5			−1.462512	−0.321764	−1.352355	−0.362743	−1.284386	−0.390342	−1.664808	−0.848713	−1.520986	−0.835652	−1.431030	−0.815251
			1.0			−1.720326	−0.272195	−1.557960	−0.316567	−1.454862	−0.348458	−1.906110	−0.838931	−1.710522	−0.824887	−1.586173	−0.803831
1.0	0.01	0.0	0.5	−0.1	−5.0	−1.463956	−0.349711	−1.353439	−0.394308	−1.285231	−0.424496	−1.666720	−0.905849	−1.522327	−0.892723	−1.432033	−0.871733
		0.1				−1.462512	−0.321764	−1.352355	−0.362743	−1.284386	−0.390342	−1.664810	−0.848713	−1.520985	−0.835652	−1.431030	−0.815251
		0.2				−1.461233	−0.298126	−1.351391	−0.335975	−1.283632	−0.361337	−1.663096	−0.800334	−1.519780	−0.787325	−1.430127	−0.767415
1.0	0.0	0.1	0.5	−0.1	−5.0	−1.462659	−0.326842	−1.352452	−0.367574	−1.284455	−0.395028	−1.664929	−0.853258	−1.521067	−0.840147	−1.431091	−0.819754
	0.2					−1.459708	−0.225442	−0.350520	−0.271067	−1.283071	−0.301403	−1.662557	−0.762445	−1.519434	−0.750339	−1.429872	−0.729769
	0.4					−1.456771	−0.124377	−1.348594	−0.174818	−1.281688	−0.207991	−1.660195	−0.671836	−1.517806	−0.660710	−1.428655	−0.639948
1.0	0.01	0.1	0.5	−0.1	−5.0	−1.462511	−0.321764	−1.352355	−0.362743	−1.284386	−0.390342	−1.664809	−0.848713	−1.520985	−0.835652	−1.431039	−0.815251
3.0						−1.486858	−0.768693	−1.370380	−0.862052	−1.298344	−0.929918	−1.689274	−1.519633	−1.538536	−1.514479	−1.444421	−1.497747
5.0						−1.501230	−1.088279	−1.380576	−1.210217	−1.306025	−1.300386	−1.703046	−1.988546	−1.548345	−1.990334	−1.451860	−1.976863
10.0						−1.522112	−1.670012	−1.395020	−1.841267	−1.316699	−1.969076	−1.723388	−2.856444	−1.562561	−2.870764	−1.462459	−2.861902
Pr	Ec	ε	Mn	β	A	$\theta_r \to -\infty$						$\theta_r = -5.0$					
						$n = 0.8$		$n = 1.0$		$n = 1.2$		$n = 0.8$		$n = 1.0$		$n = 1.2$	
						$f''(0)$	$\theta'(0)$	$f''(0)$	$\theta'(0)$	$f''(0)$	$\theta'(0)$	$f''(0)$	$\theta'(0)$	$f''(0)$	$\theta'(0)$	$f''(0)$	$\theta'(0)$
1.0	0.01	0.1	0.5	−0.1	0.0	−1.308347	−0.345998	−1.224784	−0.386147	−1.174996	−0.413076	−1.462512	−0.321764	−1.352355	−0.362743	−1.284386	−0.390342
					0.1	−1.341323	−0.481269	−1.253763	−0.505069	−1.201195	−0.518453	−1.505132	−0.466097	−1.387848	−0.489421	−1.315326	−0.502501
					0.2	−1.374175	−0.594555	−1.282418	−0.605724	−1.226941	−0.608272	−1.546427	−0.583971	−1.422296	−0.594285	−1.345337	−0.596183
					0.3	−1.406844	−0.691789	−1.310728	−0.693302	−1.252240	−0.687079	−1.586686	−0.683694	−1.455898	−0.684328	−1.374568	−0.677375
					0.4	−1.439278	−0.777376	−1.338677	−0.771281	−1.277099	−0.757773	−1.626109	−0.770762	−1.488769	−0.763866	−1.403112	−0.749645
					0.5	−1.471440	−0.854360	−1.366251	−0.842011	−1.301526	−0.822276	−1.664808	−0.848713	−1.520986	−0.835652	−1.431030	−0.815251

A and power-law index n for zero and non-zero values of fluid viscosity parameter θ_r are shown in Fig. 8 and some of them are recorded in Table 3. Fig. 8 shows that for different values of A and n, the values of $f''(0)$ are negative: This means that the surface exerts a drag force on the fluid. As n increases, the skin friction at the sheet increases. It is observed from Table 3 that for a fixed value of n the Nusselt number decreases as unsteady parameter A increases. This is true even in the presence of fluid viscosity parameter θ_r. Increase in θ_r is to decrease the skin friction and to enhance the Nusselt number as shown in Fig. 8. From Table 3, we also analyze that the effects of the fluid viscosity parameter and the magnetic parameter is to decrease the skin friction and to enhance the wall-temperature gradient. The effect of the unsteady parameter and the Prandtl number is to reduce both the surface velocity gradient and the wall-temperature gradient. The effect of heat source/sink parameter, Eckert number is to increase the wall-temperature gradient. Further, the effect of the power-law index is to enhance the skin friction and to reduce the wall-temperature gradient. This behavior holds even in the presence of fluid viscosity parameter. All the results obtained here are consistent with the physical situations.

5. Conclusion

From the numerical results obtained, some of the interesting conclusions are as follows:

1. The effect of the variable viscosity parameter and the magnetic parameter is to reduce the velocity boundary layer thickness, whereas to enhance the thermal boundary layer thickness. This observation holds for all values of the power-law index.
2. The effect of the unsteady parameter is to reduce the velocity as well as the thermal boundary layer thickness, even in the presence of variable fluid parameters.
3. The effects of the variable thermal conductivity parameter, the heat source/sink parameter and the Eckert number are to enhance, whereas the effect of the Prandtl number is to reduce the thermal boundary layer thickness. This observation is true even in the presence of the unsteady parameter.
4. Of all the parameters, the variable thermo-physical property parameters have strong effects on the skin friction, the heat transfer characteristics, the horizontal velocity component, and the temperature field.

Acknowledgements

The authors appreciate the constructive comments of the reviewers which led to definite improvement in the paper.

References

[1] Sakiadis BC. Boundary layer behavior on continuous solid surfaces. I. Boundary layer equations for two dimensional and axisymmetric flow. AIChE J 1961;7:26–8.
[2] Crane LJ. Flow past a stretching plane. Z Angew Math Phys 1970;21:645–7.
[3] Chakrabarti A, Gupta AS. Hydromagnetic flow and heat transfer over a stretching sheet. Q Appl Math 1979;37:73–8.
[4] Grubka LG, Bobba KM. Heat transfer characteristics of a continuous stretching surface with variable temperature. ASME J Heat Transfer 1985;107:248–50.
[5] Chen CK. Laminar mixed convection adjacent to vertical continuously stretching sheets. Heat Mass Transfer 1988;33:471–6.
[6] Anjali Devi SP, Thyagarajan M. Steady non-linear hydromagnetic flow and heat transfer over a stretching surface of variable temperature. Heat Mass Transfer 2006;42:671–7.
[7] Vujannovic B, Status AM, Djukiv DJ. A variational solution of the Rayleigh problem for power-law non-Newtonian conducting fluid. Ing-Arch 1972;41:381–6.
[8] Andersson HI, Bech KH, Dandapat BS. Magnetohydrodynamic flow of a power law fluid over a stretching sheet. Int J Nonlinear Mech 1992;72:929–36.
[9] Cortell R. A note on magnetohydrodynamic flow of a power-law fluid over a stretching sheet. Appl Math Comput 2005;168:557–66.
[10] Howell TG, Jeng DR, Dewitt KJ. Momentum and heat transfer on a continuous moving surface in a power law fluid. Int J Heat Mass Transfer 1997;40:1853–61.
[11] Elbashbeshy EMA, Bazid MAA. Heat transfer over an unsteady stretching surface with internal heat generation. Appl Math Comput 2003;138:239–45.
[12] Abd El-Aziz M. Radiation effect on the flow and heat transfer over an unsteady stretching sheet. Int Commun Heat Mass Transfer 2009;36:521–4.
[13] Mukhopadhyay S. Unsteady boundary layer flow and heat transfer past a porous stretching sheet in the presence of variable viscosity and thermal diffusivity. Int J Heat Mass Transfer 2009;52:5213–7.
[14] Sheikholeslami M, Ganji DD. Heat transfer of Cu–water nanofluid flow between parallel plates. Powder Technol 2013;235:873–9.
[15] Sheikholeslami M, Ashorynejad HR, Domairry G, Hashim I. Flow and heat transfer of Cu–water nanofluid between a stretching sheet and a porous surface in a rotating system, Article ID 421320. J Appl Math 2012:1–18.
[16] Abd El-Aziz M, Salem AM. MHD-mixed convection and mass transfer from a vertical stretching sheet with diffusion of chemically reactive species and space-or temperature-dependent heat source. Can J Phys 2007;85(4):359–73.
[17] Herwig H, Wickern G. The effect of variable properties on laminar boundary layer flow. Warme-und Staffubertr 1986;20:47–57.
[18] Lai FC, Kulacki FA. The effect of variable viscosity on convective heat transfer along a vertical surface in a saturated porous medium. Int J Heat Mass Transfer 1990;33:1028–31.
[19] Ali ME. The effect of variable viscosity on mixed convection heat transfer along a vertical moving surface. Int J Therm Sci 2006;45:60–9.
[20] Prasad KV, Pal Dulal, Datti PS. MHD flow and heat transfer in the flow of a power law fluid over a non-isothermal stretching sheet. CNSNS 2009;14:2178–89.
[21] Savvas TA, Markatos NC, Papaspyrides CD. On the flow of non-Newtonian polymer solutions. Appl Math Model 1994;18:14–22.
[22] Salem SM, Abd El-Aziz Mohamed M, EmadAbo-Eldahab M, Abd-Elfatah Ibrahim. Effect of variable density on hydromagnetic mixed convection flow of a non-Newtonian fluid past a moving vertical plate. CNSNS 2010;15:1485–93.
[23] Denier JP, Dabrowski PP. On the boundary layer equation for power law fluid. Proc R Soc Lond Ser A 2004;460:3143–58.
[24] Cebeci T, Bradshaw P. Physical and computational aspects of convective heat transfer. New-York: Springer-Verlag; 1984.

K. Vajravelu is a Professor of Mathematics; and Mechanical, Materials and Aerospace Engineering;University of Central Florida, Orlando, Florida 32816-1364, USA. He is teaching at the University of Central Florida since 1984. He received fourTeaching Incentive Program (TIP) Awards. He also received a Scholarship of Teaching and Learning Award (SoTL) of the University of Central Florida in April 2007. This SoTL award is based on the value and the impact of Scholarship of Teaching and Learning efforts both within the discipline and to the teaching and learning communities. Furthermore, he received two Excellence in Undergraduate Teaching Awards, College of Arts and Sciences, University of Central Florida, February 1998, and April 2002. Professor K. Vajravelu published more than 140 reasearch papers in reputed science and engineering journals published by Springer, Elsevier, Wiley, and Cambridge University Press. He also, published ''Differential Equations and Nonlinear Mechanics'' (edited), Kluwer Academic Publishers, Boston, Massachusetts (2001), 417 pages. Moreover, he is the founding Editor-in-Chief of the journal ''Differential Equations and nonlinear Mechanics,'' and editorial board member of several National and International Journals. Professor K. Vajravelu works in the areas of Applied Mathematics, Computational Fluid Mechanics, and Heat Transfer.

K. V. Prasad received a Gold Medal for Excellence in academic performance during his Master's program at Gulbarga University, Gulbarga, Karnataka, India. He obtained his Ph.D. degree in the field of Applied Mathematics from the same university during the year 2001. He has published 50 papers in research journals brought out by Springer and Elsevier publishers and his research contribution thus far has a total impact factor of 37.01. The total citation of his papers as per Google scholar exceeds 400. His research interest include free, forced, and mixed convection problems involving stretching sheet, flat plate, flow past a wedge, thin films, nanofluids, multi-layer fluid flows and porous media problems. He has research experience with Newtonian and non-Newtonian fluids. He is a reviewer for several International journals. He is a recipient of the prestigious BOYSCAST Fellowship of the Department of Science and Technology, Technology Bhavan, Government of India. As a result of this he was able to spend one year at the University of Central Florida, Orlando USA and did collaborative research with Prof. K. Vajravelu. He is presently working as a Professor in the Department of Mathematics, Vijayanagara Sri Krishnadevaraya University, Bellary, Karnataka, India. He has a teaching experience of 11 years and a research experience of 15 years.

P. S. Datti, is a Professor of Mathematics in Tata Institute of Fundamental Research, Centre for Applicable Mathematics, Bangalore, India. He obtained his Ph.D. from Courant Institute of Mathematical Sciences, New York University, New York, in 1985. Joined the T.I.F.R. Centre in 1976 as a graduate student and was on deputation to Courant Institute for pursuing higher studies; after returning in 1985, held different positions in T.I.F.R. Centre, Bangalore over the years. He has published many research papers in good journals published by Springer and Elsevier and his research contribution thus far has gained a good impact factor. His research interest include linear and nonlinear partial differential equations of evolution type: global existence and blow-up results; construction of approximate solutions via geometrical optics and other methods. Study of such equations and related ones, including ordinary differential equations as well, as dynamical systems; stability analysis. Nonlinear hyperbolic conservation laws and related topics. Boundary layer phenomena in Newtonian and non-Newtonian fluids.

Raju B T, completed his master degree at Bangalore University, Karnataka, India. He is pursuing Ph.D in the field of Applied Mathematics from Bangalore University registered in January 2009. He is presently working as Assistant Professor in REVA Institute of Technology and Management, Bangalore, India. He has a teaching experience of 9 years and a research experience of 4 years.